Investigation in the Variations of Ionospheric f_0F_2 due to Sunspot Numbers over Wakkanai using EDA Technique

Muzammil Mushtaq Hussain[1,*], Syed Nazeer Alam[2] and Faisal Ahmed Khan Afridi[3]

[1]*Institute of Space and Planetary Astrophysics (ISPA), University of Karachi, Karachi-75270, Pakistan*

[2]*Department of Electronics and Power Engineering, PNEC-National University of Sciences & Technology, Karachi, Pakistan*

[3]*Institute of Space and Planetary Astrophysics (ISPA), University of Karachi, Karachi-75270, Pakistan*

Abstract: In this research article, the authors have implemented the Exploratory Data Analysis (EDA) techniques to examine the deviation of the monthly median noon and midnight values of the critical frequency of F_2 layer ionosphere (i.e. f_0F_2) at the Wakkanai station (45.39°N, 141.68°E), Japan, during sunspot cycle 21st (1976-1986) and 23rd (1996-2008). Primarily, univariate analysis has been done, which shows the variations in f_0F_2 at different local times, seasons and in the range of sunspot numbers (SSN), in which winter and semi-annual anomalies are detected in the months of December and March respectively. Secondly, the regression analysis is being used as a bivariate data analysis. The results proved a significantly nonlinear relationship exists between f_0F_2 and SSN. In both solar cycles, saturation effects are seen in the month of March during the noontime period and immensely in June during the midnight time. The behavior of the ionosphere has been studied for different latitudes, seasonal effects and sunspot dynamic conditions, in which this paper plays an essential role in it.

Keywords: Sunspot number, Ionosphere, f_0F_2, Winter anomaly, Semi-annual anomaly, Saturation effect.

INTRODUCTION

The upper part of the Earth's atmosphere begins around from 50 to 600 kilometers, where the neutral components coexist with ionized particles and it is called the Ionosphere. This region has been affected by the intense solar natural radiation, such as Extreme Ultraviolet (EUV) rays, X-rays, gamma rays, cosmic rays and supernovae emissions that are responsible for the establishment of the ionosphere. Due to fluctuation in the ionosphere constituents i.e., temperature, density and average kinetic energy; the nature has divided this portion of the atmosphere into four layers such as D, E, F_1 and F_2. The F_2 layer is a prominent one because it persists all the time in any kind of solar or terrestrial conditions and responsible for long haul communication [1]. It is our motive to study ionospheric characteristics and processes under different conditions of solar activity. But it is not always possible to direct measured EUV radiations coming from the Sun, that is the main source of ionization in the region of the ionosphere. So researchers have to depend on solar proxies, in this scenario the Sun's most evident temporary features, i.e., sunspot numbers, which are one of the best representation of solar activity [2-4], also the other advantages of sunspot numbers are the longest available data and easy to measure.

The variability of the solar activity causes enormous variations in the density of particles, temperature, neutral winds, electric fields and other parameters in the ionosphere [5, 6]. The solar activity reliance on the F_2 layer's critical frequency of the Ionosphere (f_0F_2) or peak electron density (NmF2) have been considered for a long time [7-9]. The relationship involving the peak electron density (NmF2) and solar 10.7 cm radio flux (F10.7) or sunspot numbers (SSN) was depicted to be linear by earlier works. A nonlinear dependence of the ionospheric parameters on solar proxies was revealed in latter learning [10-12]. Then further investigations confirmed that the solar activity has an effect on the ionosphere which can be well represented by a quadratic pattern [13]. A higher-order polynomial does not effectively improve the fitting among solar activity and ionospheric parameters [14].

In our univariate analysis, we used some descriptive statistics and the graphical techniques such that the histogram and box plots were analyzed on the parameter of monthly median hourly f_0F_2 values. The bivariate data were also analyzed by using the regression plots between sunspot numbers and f_0F_2 parameters. In this paper, primarily, we show the effect of the different range of sunspot numbers on the noontime f_0F_2, secondly, observing the seasonal effects on f_0F_2. Finally, analyzed the effect of the sunspot numbers on the noon and midnight values of f_0F_2 in the months of March, June, September and December. These months are crucial when the solar zenith angle

*Address correspondence to this author at the Institute of Space and Planetary Astrophysics (ISPA), University of Karachi, Karachi-75270, Pakistan;
Tel: +4915217141800; E-mail: mushtaq@stud.uni-heidelberg.de

ISSN: 1814-8085 / E-ISSN: 1927-5129/17

is taken into account. As we know that, solar zenith angle is same at the equinoxes (i.e., March and September) while the maximum and minimum in winter (December) and summer (June) respectively. From the literature survey, we have found that ionospheric parameters over Wakkanai in 45° N latitude are not fully explored for relating sunspot dynamics with f_0F_2.

METHODOLOGY

The data on the relative sunspot number are given by the Royal Observatory of Belgium acquired from Solar Influence Data Center [15], situated in Uccle, Belgium. It has the latitude and longitude in geographical coordinates are 50.798°N and 4.358°E respectively. The relative sunspot numbers data were calculated from the observations provided from different observatories. The instrument Uccle Solar Equatorial Table (USET) is used by the Royal Observatory of Belgium to carry out spot observations. On the other hand, the data of f_0F_2, in the unit of Mega Hertz (MHz), are granted by "World Data Center for Ionosphere and Space Weather, Tokyo, National Institute of Information and Communications Technology", carried out from Ionosonde station in Wakkanai, located in the mid-latitude region in Japan, through the technique of Vertical sounding. The geographic position of Wakkanai station is 45.39°N and 141.68°E.

The monthly mean relative sunspot number data are utilized for the solar cycle 21 and 23, whilst the monthly median hourly f_0F_2 values are utilized from 1976-1986 and 1996-2008 for investigation. Previously, the comparison between the mean and median data values have been used by Chen *et al*., (2000) [11] and Yadav *et al*., (2010) [16]. The hourly data of f_0F_2 observed in the Japanese standard time (JST) (JST = Universal Time + 9 hours). We have used Spyder (Python 2.7) and Minitab 16 for data analyses.

RESULTS AND DISCUSSION

Exploratory Data Analysis

Exploratory data analysis is an approach for data analysis which utilizes the variety of techniques, mostly based on graphs, for deep understanding a data set, extract important variables, detect outliers and develop models. EDA is a perspective that how we divide a data set, what important points we should look for, how we can examine it, and how we deduce the data. For analyzing, the data can be split into two components: quantitative and graphical. A set of statistical dealings that yield numeric or tabular output are called quantitative techniques, secondly the graphical method are techniques to analyze the data through graphs. Most EDA techniques are graphical in nature which explains the structure of a data set in further detail and reveals the data's secret pattern, than the quantitative techniques [17].

Univariate Analyses

Histograms of monthly median noontime f_0F_2 of twelve months are shown in Figure **1a**, **b** for solar cycle 21st (1976-1986) and 23rd (1996-2008) respectively. Figure **1a**, **b** is further divided into three panels and each panel represents the corresponding f_0F_2 at different sunspot number range (i.e., when sunspot numbers are less than 20, while sunspot numbers are greater than 20 but lesser than 100, whilst sunspot numbers are larger than 100) [18, 19]. These figures illustrate that how much different ranges of sunspot numbers affect the f_0F_2. The f_0F_2 data are near to symmetric at high sunspot numbers while much asymmetric is seen at moderate sunspot numbers during both solar cycles.

The statistical evaluation of parametric values is mentioned in the Table **1**. In both solar cycles, it can be observed that if sunspot numbers are low, then the f_0F_2 is much confined (i.e., the mean of the coefficient of variation is around 13.5%) into smaller values, i.e., the mean value is around 6 MHz, while if sunspots are moderate in numbers, the values of f_0F_2 scattered more (i.e., mean of the coefficient of variation is about 24.4%) but the mean value is in the region of 8 MHz and beyond this, the f_0F_2 is restricted into some extent, i.e., the approximate mean of 10.5 MHz. Whilst also the minimum and maximum values of f_0F_2 showing some similarities in both solar cycles. The major source of photo-ionization process in F_2 layer is solar EUV radiations [1]. The variability in the Solar radiation emission is due to the strong magnetic field nearer to the sunspots on the Sun which dominates the emission in the high energy range of the solar spectrum, i.e., ultraviolet and X-rays [20].

In Table **1**, Positive skewness or Right skewed can be found in f_0F_2 when SSN are low and moderate, where higher values of skewness in moderate SSN show that the few values of f_0F_2 reached to higher level i.e., over 12 MHz. While the Negative skewness or Left skewed found when SSN are greater, which indicates that only few f_0F_2 values contacted with a smaller range

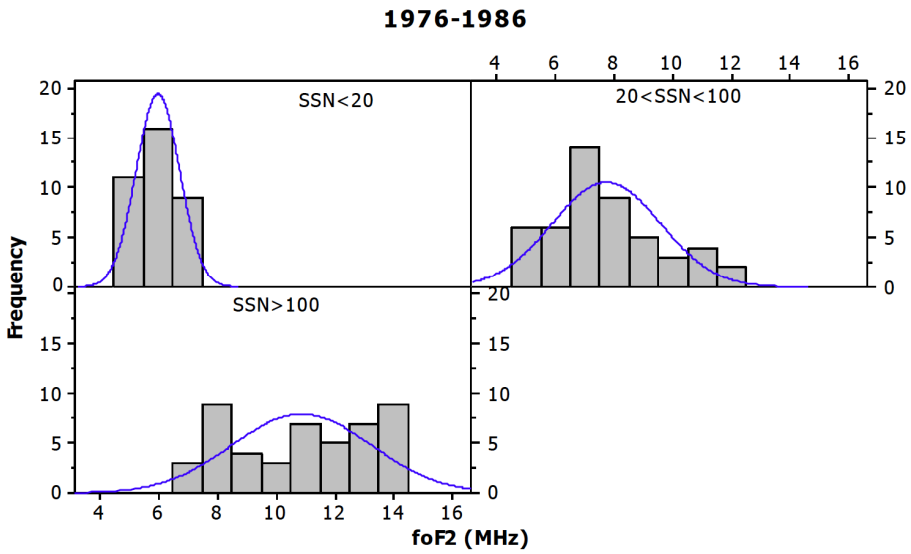

(**a**)

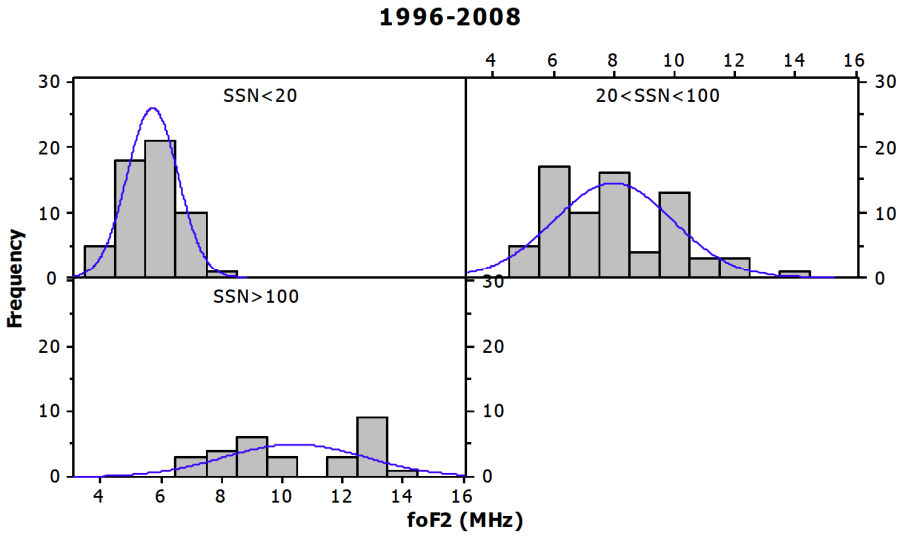

(**b**)

Figure 1: (**a**): Histogram of monthly median noontime f_0F_2 at different Sunspots range of the 21st solar cycle. (**b**): Histogram of monthly median noontime f_0F_2 at different Sunspots range of the 23rd solar cycle.

Table 1: Statistics of Noon Time f_0F_2 (MHz) at Different Sunspot Ranges

	When SSN<20		When 20<SSN<100		When SSN>100	
	21st solar cycle	23rd solar cycle	21st solar cycle	23rd solar cycle	21st solar cycle	23rd solar cycle
Mean	5.99	5.73	7.73	7.95	10.87	10.43
Coeff.Var.	12.30	14.67	23.98	24.86	21.72	22.31
Min	4.9	4.1	4.85	4.75	6.6	6.839
Max	7.45	7.8	12.2	13.7	14.4	14.25
Skewness	0.21	0.17	0.65	0.66	-0.2	-0.05
Kurtosis	-0.77	-0.36	-0.19	-0.15	-1.34	-1.57

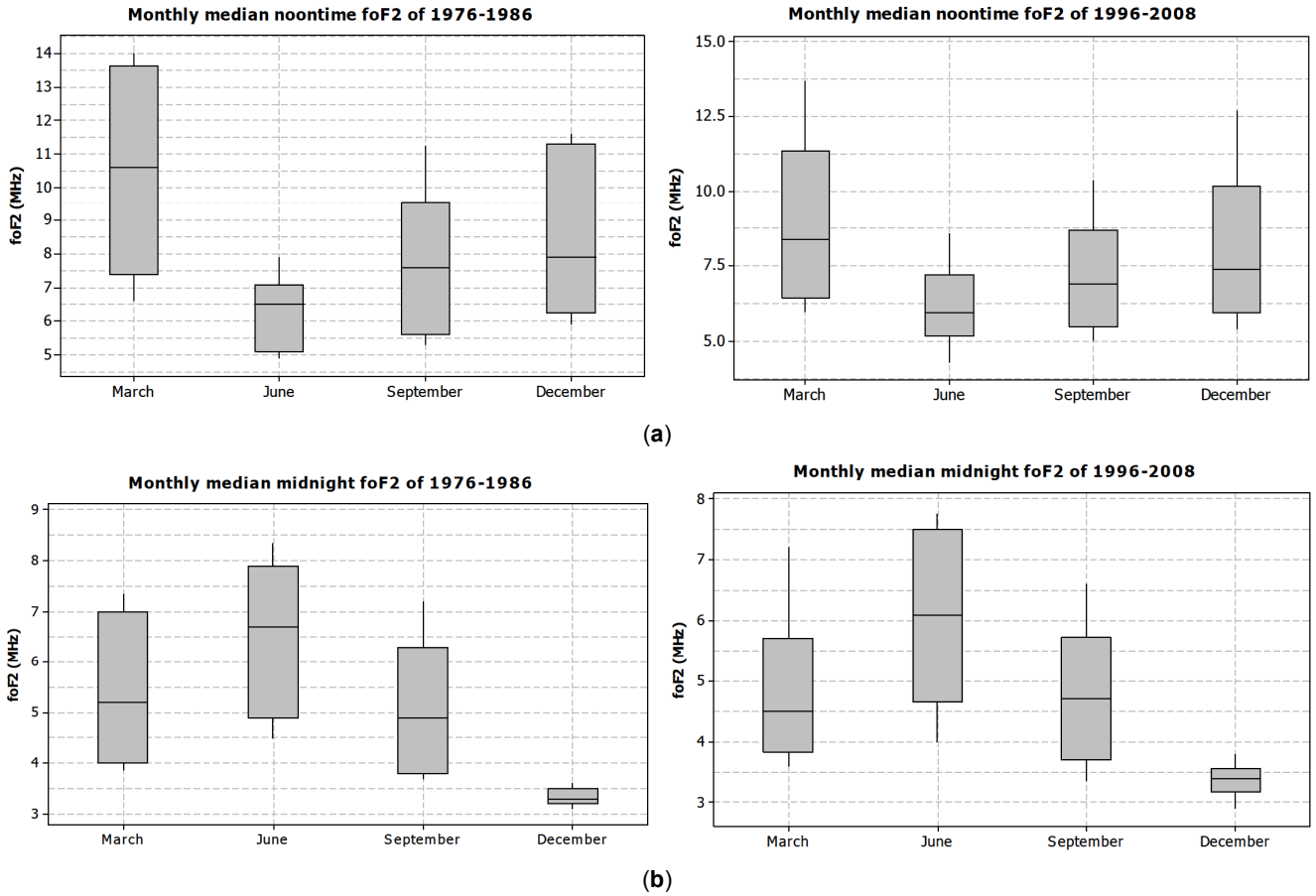

Figure 2: (**a**): Box plots of monthly median noontime values of f_0F_2 for given months for the 21st and 23rd solar cycles. (**b**): Box plots of monthly median midnight time values of f_0F_2 for given months for the 21st and 23rd solar cycles.

i.e., at around 6 MHz. Finally, for all SSN ranges, kurtosis shows negative values (i.e., platykurtic distribution), which demonstrate that f_0F_2 have flatness to the peak, and has slight tails. The more flattening in f_0F_2 can be seen when SSN is greater.

Further exploration and information can be extracted by using box plots as seen in Figure **2a**, **b**. Box plots can be used to illustrate the quartiles information and outlier detection of the data. The variation in f_0F_2 can be evidently seen at different local times and in seasons i.e., different months.

The Figure **2a** shows the monthly median noon time values of f_0F_2 during the months of March, June, September and December for the 21st solar cycle (1976-1986) and 23rd solar cycle (1996-2008). For both solar cycles, box plot has highest height in the month of March. Second and third highest box plots are in the months of December and September respectively, while the lowest height in the month of June. The same interpretations are for the maximum, minimum, median and inter-quartile range (IQR) values of f_0F_2 at noon time for both solar cycles. Seasonal behavior of f_0F_2 that deviate from solar zenith angle dependence, are categorized into winter and semi-annual anomalies. Winter anomaly is those where electron densities (or f_0F_2) is higher in winter i.e., December, than in the summer i.e., June, at daytime, whereas semi-annual anomaly are those in which f_0F_2 is larger in equinoxes than in solstice, which can be seen in the box plots of December and March.

The reason of semi-annual anomaly is the asymmetric hemispheric heating of the atmosphere in the period of solstices, which stimulates the global scale interhemispheric thermospheric circulation [21, 22]. In this condition heavy molecular gases are moved up and their density amplifies in the F region, which decrease in the atomic oxygen and molecular nitrogen ratio (i.e., O/N_2), during the summer solstice in mid-latitude. The solar heating is symmetric in equinoxes and the stormy mixing is relatively weaker as compared to summer solstice. As a result, the O/N_2 ratio is greater during equinox than during the summer solstice and creates the semi-annual anomaly in thermospheric neutral composition [21].

The winter anomaly is known to be linked with the seasons and variations in thermospheric neutral composition [23-25]. The summer-to-winter wind circulation, stimulates different thermospheric neutral compositions between summer and winter. In summer, molecular gases raises in the F region, which increases the reaction of O^+ with molecular gases, resulting decrease in the density of plasma. The reverse process takes place in winter, resulting increase in the density of plasma.

However box plots for midnight time as illustrated in Figure **2b** which shows that for both solar cycles, box plot is highest in level in the month of June which illustrate the opposite behavior from noontime. Second and third highest level of box plots are in March and September respectively, while December has lowest in level. Around the same information are for the maximum, minimum, median and inter-quartile range (IQR) values of f_0F_2 at midnight time for both solar cycles.

Comparison between noon and midnight f_0F_2 clearly shows that values of f_0F_2 are towering in noontime due to the solar EUV radiations shown in Figure **2a**, although at midnight time all given months showing low values except for the month of June where the values of f_0F_2 around similar as shown in Figure **2b**, this is due to the effect called Mid-latitude Summer Nighttime Anomaly (MSNA). This is the combined phenomena of neutral wind and the geomagnetic configuration in which during daytime (around noon) the electron density are low and fluctuate slightly but at pre-midnight (~22:00 LT) electron density enhance and decline at post-midnight (~04:00 LT). Because at nighttime, the upward wind lifted the ionosphere up to regions of lower recombination rate, although during daytime strong downward wind tends the ionosphere up to regions of high recombination rate [9, 26].

Bivariate Data Analyses

In order to find out the dependence of ionization of F_2 layer on the sunspots, regression analysis have been executed between f_0F_2 and the sunspot numbers. Previously done researches show that the saturation effect could not be explained by linear fitting, so quadratic fitting were used instead [27-29].

$$f_0F_2 = a_0 + a_1 \times SSN + a_2 \times (SSN)^2$$

Where, a_0, a_1 and a_2 are the coefficients of the quadratic regression fit. The term a_2 has its importance, when $a_2 < 0$, indicates that f_0F_2 declines with increasing sunspot numbers which represents the saturation effect. Whilst $a_2 > 0$ signify that f_0F_2 increases with the number of spots increases.

Δf_0F_{2max} parameter is used to determine the effect of the different magnitude of solar cycles on f_0F_2. Δf_0F_{2max} has been calculated by deducting the highest values of f_0F_2 acquired from the two solar cycles [16].

Δf_0F_{2max} = f_0F_{2max} (for 21st solar cycle) - f_0F_{2max} (for 23rd solar cycle)

The maximum noontime value of f_0F_2 is around 8-14 MHz for 21st solar cycle while it is about 8-13 MHz for the 23rd solar cycle. During the midnight time, the maximum f_0F_2 values are in the region of 3-8 MHz for the solar cycle 21st whilst around 4-7 MHz for the 23rd solar cycle. Result of Table **2** could attribute that the different magnitude of solar activity affects less in March where the semi-annual anomaly play a main role for ionization. While in September, different magnitude of solar activity affects noticeable on both the noon and midnight time f_0F_2 values. However, in December at noontime, the negative value is due to the saturation effect on high sunspot numbers and in June at midnight, the strong influence of the magnitude of solar activity on f_0F_2 values clearly seen.

Table 2: Compute Δf_0F_{2max} for Different Months at Noon and at Midnight Time for the Solar Cycle 21 and 23

Months	Time (JST)	21st Solar cycle f_0F_{2max} (MHz)	23rd Solar cycle f_0F_{2max} (MHz)	Difference Δf_0F_{2max} (MHz)
March	0000	7.35	7.2	0.15
	1200	14	13.7	0.3
June	0000	8.35	7.75	0.6
	1200	7.9	8.6	-0.7
September	0000	7.2	6.6	0.6
	1200	11.25	10.388	0.826
December	0000	3.6	3.8	-0.2
	1200	11.6	12.7	-1.1

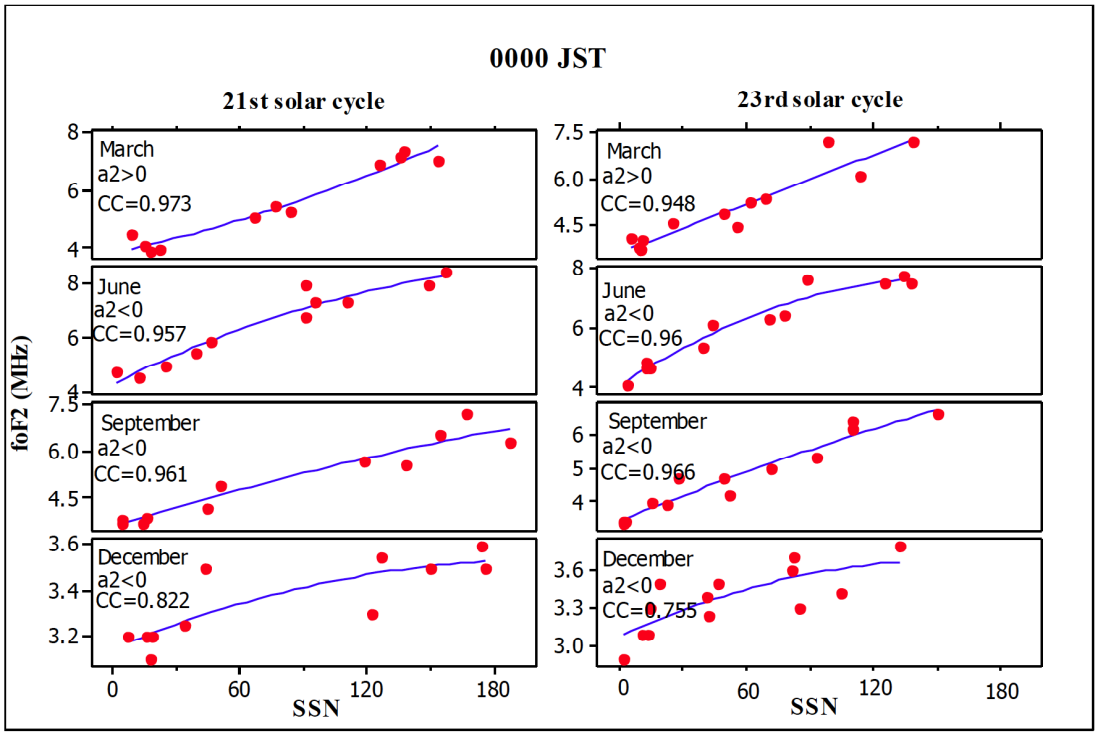

(**a**)

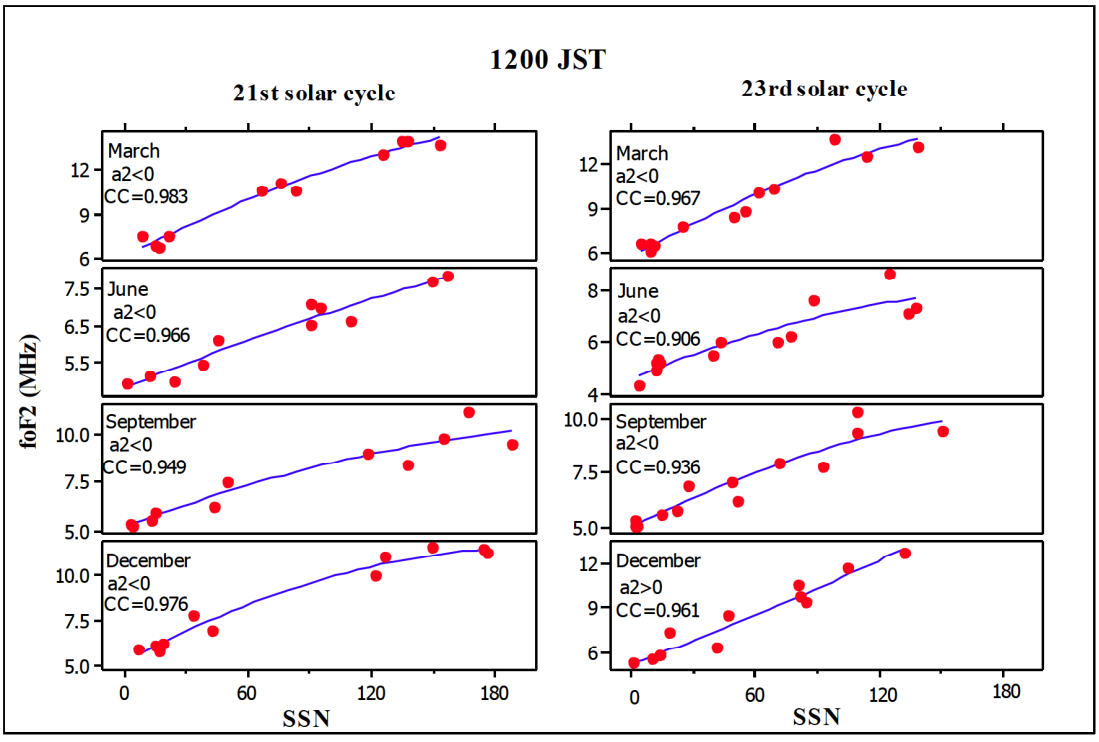

(**b**)

Figure 3: (**a**): Regression plots between f_0F_2 and SSN at midnight time period during the 21st and 23rd solar cycles. (**b**): Regression plots between f_0F_2 and SSN at noontime period during the 21st and 23rd solar cycles.

The Figure **3a**, **b** shows the behavior of f_0F_2 over Wakkanai during noon and midnight time. It can be distinguished that at noontime, f_0F_2 values remain roughly constant for March and December at maximum spot numbers in the 21st solar cycle. Similar behavior is observed in the 23rd solar cycle in March, June and September, which shows the saturation effect of high sunspot number. During the midnight time, saturation is

seen immensely in June and slightly in December of both solar cycles. Beside from saturation, the clear upward trend is observed in the month of March at midnight time during the 21st solar cycle and also in December at noontime during the 23rd solar cycle.

Pearson correlation (CC) in noon time is higher in the 21st solar cycle for each given month, while it is slightly lower in the 23rd solar cycle. And for all given months in noon and at midnight the correlation coefficients are strongly positive for both the solar cycles except in the month of December at midnight for the 23rd solar cycle in which the relationship between sunspot number and f_0F_2 is less strongly positive.

The saturation effect is especially the result of the changing in neutral O/N_2 concentration ratio. N_2 is a major constituents taking part in the recombination process in the ionosphere [30]. The ratio of O/N_2 depends on the solar zenith angle, the immense aspect about this ratio is the huge decrease with solar activity for winter, when the solar zenith angle is maximized at 45° latitude [31]. It is due to non-uniform expansion of atmospheric constituents in response of absorption of EUV radiation [32]. The scale height of N_2 increases appreciably than atomic oxygen scale height as the sunspot number approaches to their maximum. The recombination process increases due to increases in the scale height of N_2. This anomalous role of N_2 enhances the recombination process, appear as a saturation effect.

CONCLUSION

Ionospheric investigation is being done for numerous years to understanding the behavior of ionosphere for different solar and seasonal circumstances. The univariate analysis shows that the range of sunspot numbers changing f_0F_2 data, which are near to symmetric at high sunspot numbers (i.e., SSN>100), while much asymmetry is found in moderate sunspot numbers (20<SSN<100) where the data of f_0F_2 are scattered more. Box plot analysis shows that, firstly, box plots are higher in noontime as compared to the midnight time. Secondly, at a noontime box plot is highest in height in the month of March. Second and third elevated box plots are in the months of December and September respectively, while the lowest height is in the month of June. Winter and semi-annual anomaly can be observed in December and March respectively because of their high values. However box plots for midnight time is highest in level in the month of June which is opposite from noontime.

Regression plots used as a bivariate data analysis explained that f_0F_2 is not linearly dependent on sunspot numbers, however the quadratic fit is better for explaining relationship instead, which represent the saturation effect accurately. The phenomenon of saturation depends on local time, seasons (different months) and on the magnitude of solar activity. The different magnitude of solar activity affects largely in the month of September while, minimum influence on March. The Correlation coefficient illustrates positive, strong relationships between f_0F_2 and SSN at noon and at midnight time, except for the month of December at midnight time during the 23rd solar cycle, which shows moderate high positive relation. The study demonstrates the modulation of ionosphere, relative to diurnal, seasonal and sunspot numbers, which improved the understanding of the ionospheric structure and its evolution for the researchers, Space agencies and Radio communication organizations.

ACKNOWLEDGEMENT

We are deeply grateful for providing the data of sunspot numbers by Royal Observatory of Belgium and ionospheric data from the World Data Center for Ionosphere and Space Weather, Tokyo, Japan.

REFERENCES

[1] Zolesi B, Cander RL. Ionospheric Prediction and Forecasting. Berlin, Germany: Springer 2014; 39-44. https://doi.org/10.1007/978-3-642-38430-1

[2] Tobiska WK, Woods T, Eparvier F, Viereck R, Floyd L, Bouwer D, *et al*. The SOLAR2000 empirical solar irradiance model and forecast tool. J Atmos Solar-Terrestrial Phys 2000; 62(14): 1233-50. https://doi.org/10.1016/S1364-6826(00)00070-5

[3] Richards PG, Woods TN, Peterson WK. HEUVAC: A new high resolution solar EUV proxy model. Adv Sp Res 2006; 37(2): 315-22. https://doi.org/10.1016/j.asr.2005.06.031

[4] Ramesh KB, Rohini VS. The Astrophysical Journal , 686: L41-L44, 2008 October 10 2008. Astrophys J 2008; 686: 41-4. https://doi.org/10.1086/592774

[5] Gorney DJ. Solar cycle effects on the near-Earth space environment. Rev Geophys 1990; 28(3): 315-36. https://doi.org/10.1029/RG028i003p00315

[6] Forbes JM, Bruinsma S, Lemoine FG. Solar rotation effects on the thermospheres of Mars and Earth. Science 2006; 312(5778): 1366-8. https://doi.org/10.1126/science.1126389

[7] Lei J, Liu L, Wan W, Zhang SR. Variations of electron density based on long-term incoherent scatter radar and ionosonde measurements over Millstone Hill. Radio Sci 2005; 40(2): 1-10. https://doi.org/10.1029/2004RS003106

[8] Liu L, Wan W, Ning B. Authors: Solar activity variations of ionospheric peak electron density. Geology 2006; 111(April): 1-13. https://doi.org/10.7312/lu--13852-004

[9] Mushtaq M, Alam SN, Afridi FAK, Ameen MA. Effects of Sunspots Cycles on Diurnal and Seasonal Trend of foF2. J Geosp Sci 2015; 1(September): 44-50.

[10] Balan N, Bailey GJ, Su YZ. Variations of the ionosphere and related solar fluxes during solar cycles 21 and 22. Adv Sp Res 1996; 18(3): 11-4. https://doi.org/10.1016/0273-1177(95)00828-3

[11] Chen YI, Liu JY, Chen SC. Statistical investigation of the saturation effect of sunspot on the ionospheric f0F2. Phys Chem Earth 2000; 25(4): 359-62.

[12] Chen Y, Liu L, Le H. Solar activity variations of nighttime ionospheric peak electron density. J Geophys Res Sp Phys 2008; 113(11): 1-11. https://doi.org/10.1029/2008ja013114

[13] Liu L, Chen Y. Statistical analysis of solar activity variations of total electron content derived at Jet Propulsion Laboratory from GPS observations. J Geophys Res 2009; 114(A10): A10311. https://doi.org/10.1029/2009JA014533

[14] Kouris SS. The solar-cycle variation of M(3000) F2 and its correlation with that of f0F2. Ann Di Geofis 1998; 41(4): 583-90.

[15] SIDC. Solar Influence Data Center. [cited 2015 May 15]. Available from: http://www.sidc.oma.be/

[16] Yadav S, Dabas RS, Das RM, Upadhayaya AK, Sarkar SK, Gwal AK. Variation of F-region critical frequency (f0F2) over equatorial and low-latitude region of the Indian zone during 19th and 20th solar cycle. Adv Sp Res 2010; 47(2011): 124-37. https://doi.org/10.1016/j.asr.2010.09.003

[17] Fleming GMC, Nellis GJ. Principles of Applied Statistics. London, UK: Routledge 1994; 65-66.

[18] Ouattara F, Amory-Mazaudier C, Fleury R, Lassudrie Duchesne P, Vila P, Petitdidier M. West African equatorial ionospheric parameters climatology based on ouagadougou ionosonde station data from june 1966 to february 1998. Ann Geophys 2009; 27(6): 2503-14. https://doi.org/10.5194/angeo-27-2503-2009

[19] Pham Thi Thu H, Amory-Mazaudier C, Le Huy M. Time variations of the ionosphere at the northern tropical crest of ionization at Phu Thuy, Vietnam. Ann Geophys 2011; 29(1): 197-207. https://doi.org/10.5194/angeo-29-197-2011

[20] Vazquez M, Hanslmeier A. Ultraviolet Radiation in the Solar System. Virginia, U.S.A: Springer 2006; 69-70. https://doi.org/10.1007/1-4020-3730-9_3

[21] Fuller-Rowell TJ. The 'thermospheric spoon': A mechanism for the semiannual density variation. J Geophys Res 1998; 103(97): 3951. https://doi.org/10.1029/97JA03335

[22] Rishbeth H, Müller-Wodarg ICF, Zou L, Fuller-Rowell TJ, Millward GH, Moffett RJ, *et al*. Annual and semiannual variations in the ionospheric F2-layer: II. Physical discussion. Ann Geophys 2000; 18(8): 945-56. https://doi.org/10.1007/s00585-000-0945-6

[23] Rishbeth H, Heelis RA, Muller-Wodarg ICF. Variations of thermospheric composition according to AE-C data and CTIP modelling. Ann Geophys 2004; 22(2): 441-52. https://doi.org/10.5194/angeo-22-441-2004

[24] Yu T, Wan W, Liu L, Zhao B. Global scale annual and semi-annual variations of daytime NmF2 in the high solar activity years. J Atmos Solar-Terrestrial Phys 2004; 66(18): 1691-701. https://doi.org/10.1016/j.jastp.2003.09.018

[25] Rishbeth H, Müller-Wodarg ICF. Why is there more ionosphere in January than in July? The annual asymmetry in the F2-layer. Ann Geophys 2006; 24(12): 3293-311. https://doi.org/10.5194/angeo-24-3293-2006

[26] Thampi SV, Balan N, Lin C, Liu H, Yamamoto M. Mid-latitude Summer Nighttime Anomaly (MSNA) - observations and model simulations. Ann Geophys 2011; 29: 157-65. https://doi.org/10.5194/angeo-29-157-2011

[27] Kane RP. Solar cycle variation of f0F2. J Atmos Solar-Terrestrial Phys 1992; 54: 1201-5. https://doi.org/10.1016/0021-9169(92)90145-B

[28] Thomas D. Xenos, Stamatis S Kouris BZ. Assessment of the solar-cycle dependence of f0F2. Ann Di Geofis 1996; XXXIX(6): 1157-66.

[29] Dabas RS, Sharma K, Das RM, Sethi NK, Pillai KGM, Mishra AK. Ionospheric modeling for short- And long-term predictions of F region parameters over Indian zone. J Geophys Res Sp Phys 2008; 113(3).

[30] Rishbeth H. How the thermospheric circulation affects the ionospheric F2-layer. J Atmos Solar-Terrestrial Phys 1998; 60(14): 1385-402. https://doi.org/10.1016/S1364-6826(98)00062-5

[31] Hedin AE, Reber CA, Spencer NW, Brinton HC, Kayser DC. Global model of longitude/UT variations in thermospheric composition and temperature based on mass spectrometer data. J Geophys Res Sp Phys 1979; 84(A1): 1-9. https://doi.org/10.1029/JA084iA01p00001

[32] Schunk RW, Walker JCG. Theoretical ion densities in the lower ionosphere. Planet Space Sci 1973; 21(11): 1875-96. https://doi.org/10.1016/0032-0633(73)90118-9

Received on 15-03-2017 Accepted on 18-04-2017 Published on 11-08-2017

https://doi.org/10.6000/1927-5129.2017.13.69